High-Performance Absorbing Boundary Conditions for Photonic Crystal Waveguide Simulations

Masanori Koshiba, *Senior Member, IEEE*, Yasuhide Tsuji, *Member, IEEE*, and Satoru Sasaki

Abstract—A high-performance absorbing boundary condition is newly developed for the reduction of spurious reflections in photonic crystal (PC) waveguide simulations. The PC waveguide is terminated with a perfectly matched layer (PML) in which the original PC structure remains as is. This PC-based PML works well, compared to a conventional PML, which acts as a homogeneous absorbing medium, simulating a semi-infinite free space and to a distributed-Bragg-reflector waveguide, which was recently developed to reduce reflections from PC waveguide ends, improving a wavenumber matching condition for PC waveguide modes.

Index Terms—Absorbing boundary condition, perfectly matched layer, photonic crystal, photonic crystal waveguide, time-domain analysis.

I. INTRODUCTION

PHOTONIC crystals (PCs) have inspired great interest because of their potential ability to control the lightwave propagation. Mekis *et al.* [1] have demonstrated high transmission through a sharp 90° bend in PC waveguides by using the finite-difference time-domain (FDTD) method. When simulating PC waveguide devices and/or circuits, in order to reduce spurious reflections from the computational window edges, the use of appropriate absorbing boundary conditions is indispensable. For this purpose, the so-called perfectly matched layer (PML) condition [2] has been applied to PC waveguide simulations [1]. Although the impedance matching condition is satisfied at the interface between the PML region and the non-PML, real PC region, substantial reflection was observed [1], [3]. Recently, Mekis *et al.* [3] have proposed to terminate a PC waveguide with a distributed-Bragg-reflector (DBR) waveguide improving the wavenumber matching condition for PC waveguide modes. However, this condition can be exactly satisfied at only one frequency, and the reflection level was still on the order of a few percent. In this paper a high-performance absorbing boundary condition for PC waveguide simulations will be presented.

We consider a two-dimensional PC waveguide ($\partial/\partial x = 0$) surrounded by PMLs of thickness d_i ($i = 1$ to 4) as shown in Fig. 1, in which the original PC structure remains as is, hereafter, referred to as PC-based PML. Using the anisotropic PML [4],
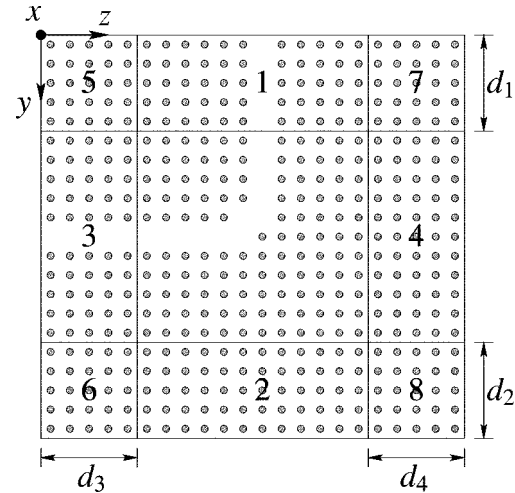
Fig. 1. Photonic crystal (PC) waveguide surrounded by PC-based perfectly matched layer (PML) regions 1 to 8.

[5], the PML permittivity and permeability tensors are written as

$$[\varepsilon]_{\mathrm{PML}} = \varepsilon_0 n^2 [\Lambda], \qquad [\mu]_{\mathrm{PML}} = \mu_0 [\Lambda] \tag{1}$$

with

$$[\Lambda] = \begin{bmatrix} s_y s_z/s_x & 0 & 0 \\ 0 & s_z s_x/s_y & 0 \\ 0 & 0 & s_x s_y/s_z \end{bmatrix} \tag{2}$$

where ε_0 and μ_0 are permittivity and permeability of free space, n is the refractive index, and the PML parameters, s_x, s_y, and s_z, are given in Table I. Assuming parabolic profiles of artificial electric and magnetic conductivities, σ and σ^*, the value of s_i in Table I is taken as

$$s_i = 1 - j(\rho/d_i)^2 \tan \delta_i \tag{3}$$

with

$$\tan \delta_i = \frac{\sigma_{i,\max}}{\omega \varepsilon_0 n_{i0}^2} = \frac{\sigma^*_{i,\max}}{\omega \mu_0} \tag{4}$$

where ρ is the distance from the beginning of PML (PML surface), δ_i is the loss angle at the end of PML ($\rho = d_i$), ω is the angular frequency, n_{i0} is the refractive index at the PML surface ($\rho = 0$), subscript "max" is the maximum value, and (4) is required to satisfy the impedance matching condition at

TABLE I
PML PARAMETERS

PML parameter	PML region							
	1	2	3	4	5	6	7	8
s_y	s_1	s_2	1	1	s_1	s_2	s_1	s_2
s_z	1	1	s_3	s_4	s_3	s_3	s_4	s_4

$s_x = 1$ in all the PML regions.

TABLE II
DEFINITION OF Φ, p, AND q

mode	Φ	p	q
TE	E_x	1	n^2
TM	H_x	$1/n^2$	1

the interface between the PML region and the real PC region $(s_x = s_y = s_z = 1)$.

From Maxwell's equations with (1) and (2), we obtain

$$\frac{\partial}{\partial y}\left(p\frac{s_z}{s_x s_y}\frac{\partial \Phi}{\partial y}\right) + \frac{\partial}{\partial z}\left(p\frac{s_y}{s_x s_z}\frac{\partial \Phi}{\partial z}\right) - \frac{s_y s_z}{s_x}\frac{q}{c^2}\frac{\partial^2 \Phi}{\partial t^2} = 0 \tag{5}$$

where c is the light velocity in free space, and Φ, p, q are defined in Table II with E_x and H_x being, respectively, the x components of the electric and magnetic fields. To solve (5) in time domain, we adopt a recently developed time-domain beam propagation method based on a finite element scheme [6] which can treat a slowly varying envelope of a pulsed wave. In the time-domain analysis, ω in (4) is regarded as a carrier center angular frequency, ω_c.

In order to quantify reflection properties when a PC-based PML is applied to a PC waveguide, we carry out numerical simulations of pulse propagation in a PC straight waveguide [3]. The waveguide is terminated with a conventional PML, a distributed-Bragg-reflector (DBR) waveguide [3], and a PC-based PML as shown, respectively, in Fig. 2(a)–(c), where dielectric rods with circular cross-section of radius $r = 0.2a$ and refractive index $n = 3.4$ are embedded in air on a square array with lattice constant a. The waveguide, which runs along the middle of the cell, at the distance of $6a$ from the edges, is designed long enough that at the cell center there is virtually no overlap between the original pulse and the pulse reflected from the waveguide end. This PC has a photonic band gap (PBG) for TE modes which extends from $\omega a/(2\pi c) = 0.283$ to 0.424, but not for TM modes. Due to the exponential decay of guided modes within PBG, the fields are very small at the cell boundaries parallel to the waveguide and thus, special care is not necessary at these boundaries.

The measured reflection coefficient is shown as a function of normalized angular frequency in Fig. 3, where the inputted TE Gaussian pulse has a carrier center angular frequency $\omega_c a/(2\pi c) = 0.368$, and the reflection amplitudes from the PC waveguide end terminated with a conventional PML, a DBR waveguide, and a PC-based PML are, respectively, calculated from FDTD [3] (also checked by using FETD-BPM), FDTD [3], and FETD-BPM.

When using a conventional PML, substantial reflection is observed on the order of 20 to 30%. When using a DBR waveguide,
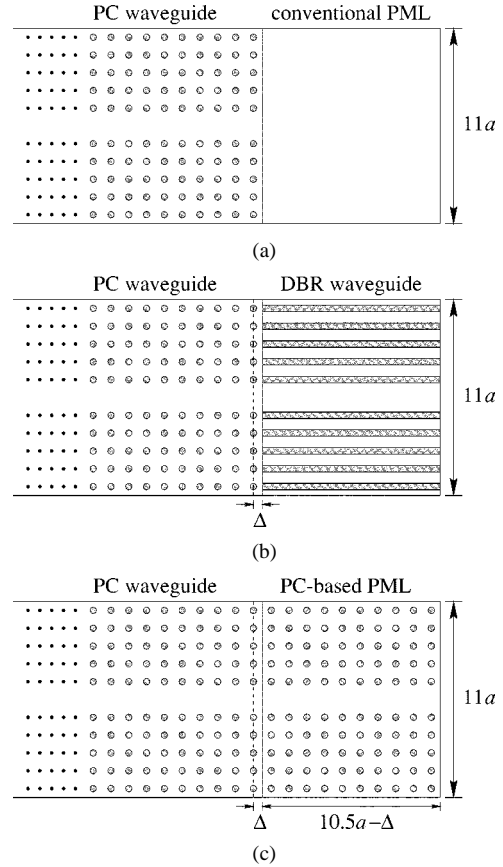

Fig. 2. PC straight waveguides terminated with (a) conventional PML, (b) DBR waveguide, and (c) PC-based PML.
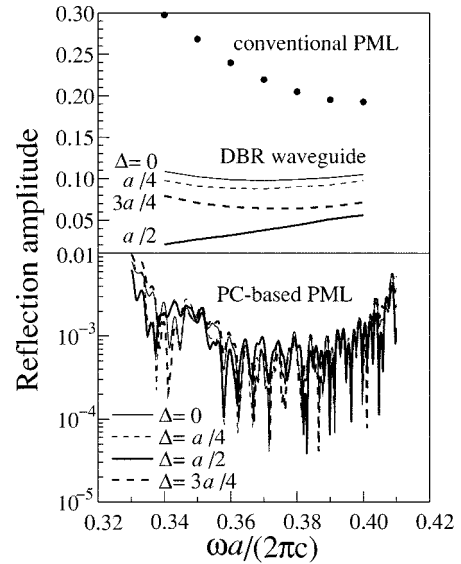

Fig. 3. Reflection amplitudes for conventional PML, DBR waveguide, and PC-based PML terminations.

there is a large improvement over the reflection from the conventional PML termination, but it is still on the order of a few percent. Also, the reflection level depends on the distance Δ between the beginning of DBR waveguide and the line defined by the centers of the last row of rods within the real PC region, and the lowest reflection is obtained for $\Delta = a/2$. When using a PC-based PML proposed here, on the other hand, the reflection
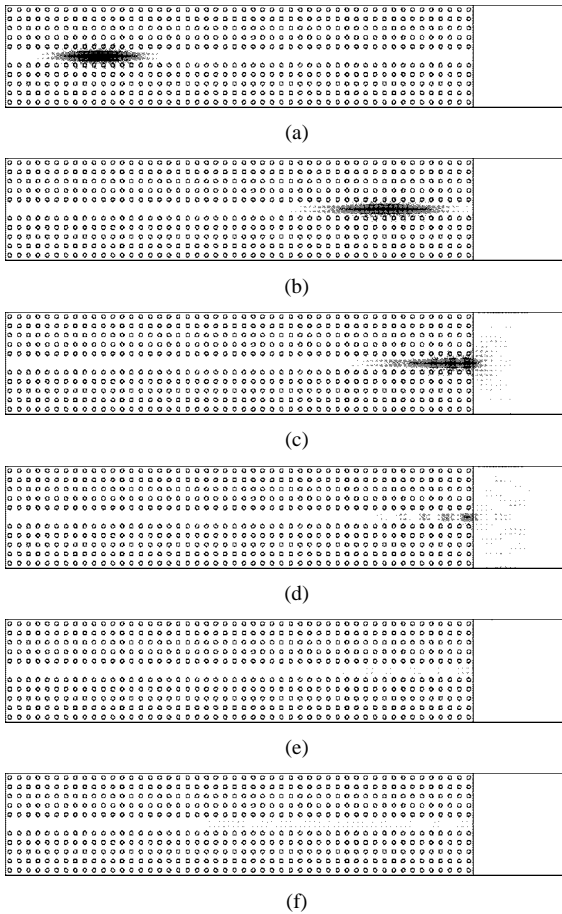
Fig. 4. Electric field patterns for conventional PML termination. (a) $t = 0$ fs (incident pulse). (b) $t = 120$ fs. (c) $t = 150$ fs. (d) $t = 180$ fs. (e) $t = 210$ fs. (f) $t = 240$ fs.
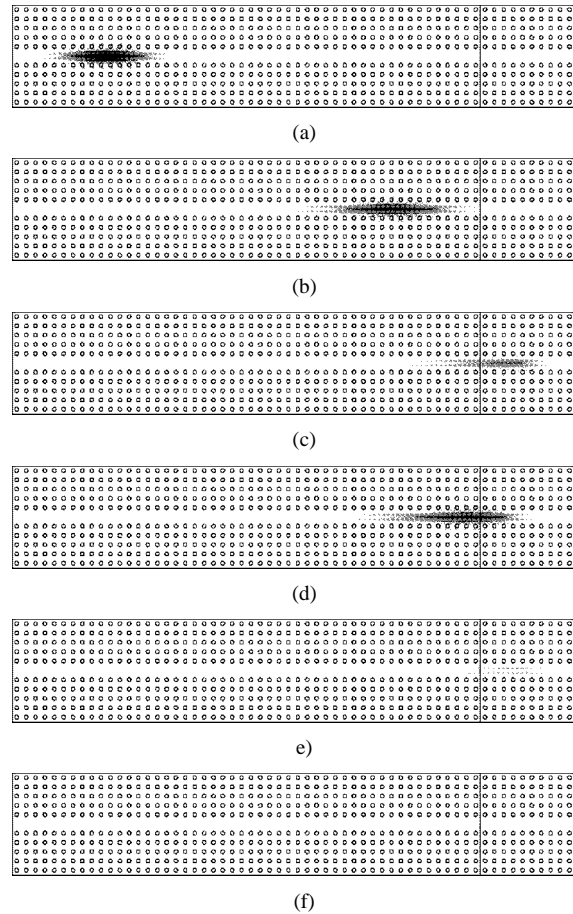

Fig. 5. Electric field patterns for PC-based PML termination. (a) $t = 0$ fs (incident pulse). (b) $t = 120$ fs. (c) $t = 150$ fs. (d) $t = 180$ fs. (e) $t = 210$ fs. (f) $t = 240$ fs.

amplitude is drastically reduced and is less than -50 dB across a wide range of frequencies, irrespective of values of Δ. It should be noted that the reflection is larger at low and high frequencies near PBG edges.

Electric field patterns for the conventional PML and the PC-based PML terminations are, respectively, shown in Figs. 4 and 5. When using a conventional PML, we can see substantial reflection from the PML surface. When using a PC-based PML, on the other hand, the reflected field can be handly observed. A PC-based PML works well, compared to a conventional PML, because pulsed waves experience the same permittivity contrast as in the real PC region. A conventional PML, on the other hand, has not such a permittivity contrast and thus, acts as a homogeneous absorbing medium. The present PC-based PML is effective not only for guided modes confined in defect regions but for nonguided, radiated fields.

In conclusion, we have proposed a high-performance PC-based PML for PC waveguide simulations. This provides a simple means for reducing spurious reflections from computa-tional window edges, compared to the conventional PML and the PBG waveguide terminations.

REFERENCES

[1] A. Mekis, J. C. Chen, I. Kurland, S. Fan, P. R. Villeneuve, and J. D. Joannopoulos, "High transmission through sharp bends in photonic crystal waveguides," *Phys. Rev. Lett.*, vol. 77, pp. 3787–3790, Oct. 1996.

[2] J.-P. Berenger, "A perfectly matched layer for the absorption of electro-magnetic waves," *J. Comput. Phys.*, vol. 114, pp. 185–200, Oct. 1994.

[3] A. Mekis, S. Fan, and J. D. Joannopoulos, "Absorbing boundary con-ditions for FDTD simulations of photonic crystal waveguides," *IEEE Microwave Guided Wave Lett.*, vol. 9, pp. 502–504, Dec. 1999.

[4] J.-Y. Wu, D. M. Kingsland, J.-F. Lee, and R. Lee, "A comparison of anisotropic PML to Berenger's PML and its application to the finite-element method for EM scattering," *IEEE Trans. Antennas Propagat.*, vol. 45, pp. 40–50, Jan. 1999.

[5] F. L. Teixeira and W. C. Chew, "General closed-form PML constitutive linear media," *IEEE Microwave Guided Wave Lett.*, vol. 8, pp. 223–225, June 1998.

[6] M. Koshiba, Y. Tsuji, and M. Hikari, "Time-domain beam propagation method and its application to photonic crystal circuits," *J. Lightwave Technol.*, vol. 18, pp. 102–110, Jan. 2000.